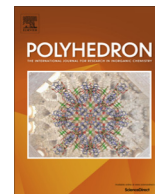




Contents lists available at ScienceDirect

Polyhedron

journal homepage: www.elsevier.com/locate/poly

Synthesis and characterization of TiL_2 complexes with tridentate (ONO) (S)-NOBIN Schiff-base ligands

Sanmitra Barman, John Desper, Christopher J. Levy*

Department of Chemistry, Kansas State University, 213 CBC Bldg., Manhattan, KS 66506, USA

ARTICLE INFO

Article history:

Received 2 April 2014

Accepted 2 July 2014

Available online xxx

Keywords:

NOBIN

Schiff-base

Titanium(IV)

Carbonyl-ene

Aldol

ABSTRACT

Tridentate (ONO) C_1 -symmetric Schiff base ligands were synthesized by the condensation of (S)-2-amino-2'-hydroxy-1,1'-binaphthalene with 4-hydroxy-3-phenanthrenecarboxaldehyde or 1-hydroxybenz[a]anthracene-2-carboxaldehyde. C_2 -symmetric titanium(IV) Schiff base complexes, TiL_2 , were synthesized and characterized with these ligands. The complex with the benz[a]anthryl unit crystallizes in a facial coordination mode, OC-6-1'3'-C, whereas complex with phenanthryl unit crystallizes in a meridional mode, OC-6-22'-A. A comparison between the complexes and the ligands were done in solution using circular dichroism spectroscopy. Preliminary catalytic studies showed that these complexes can catalyze asymmetric carbonyl-ene addition reactions of 2-methoxypropene with aromatic aldehydes with moderate selectivity. The ligands and complexes were characterized by NMR, HRMS, single crystal X-ray diffraction and CD spectroscopy.

© 2014 Elsevier Ltd. All rights reserved.

1. Introduction

Carbon–carbon bond formation by asymmetric aldol additions and carbonyl-ene reactions are widely used in organic synthesis and the pharmaceutical industry. These transformations are effective for producing chiral β -hydroxy aldehydes or β -hydroxy ketones [1], and considerable effort has been directed to the development of new organo- and transition metal catalysts for a variety of important substrates [2]. Effective catalysts for aldol and related hetero-ene reactions based on Ti(IV) Lewis acids with NOBIN (2-amino-2'-hydroxy-1,1'-binaphthyl) derived Schiff-base ligands were first developed by Carreira (Scheme 1) [3]. The titanium complex (R)-2 derived from ligand (R)-1 is sufficiently electrophilic to activate aldehydes towards the addition of weak nucleophiles such as 2-methoxypropene under mild conditions. Subsequently, the NOBIN moiety has received considerable interest as the chiral component of asymmetric catalysts [4]. Despite their significance, few transition-metal NOBIN complexes have been structurally characterized [5,6]. Herein we report two new NOBIN-based Schiff-base ligands with extended aromatic sidearms containing phenolate-type donors in phenanthryl or benz[a]anthryl ring structures. TiL_2 X-ray structures are reported and catalytic activity is examined for the addition of 2-methoxypropene to aryl aldehydes.

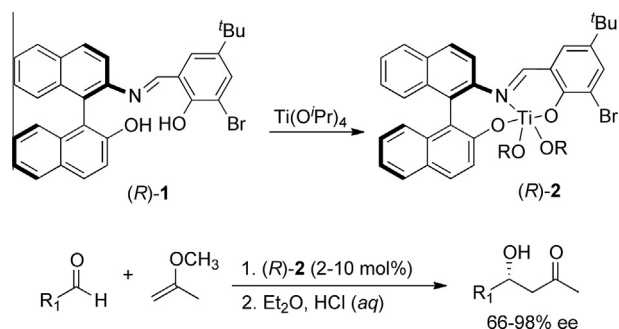
2. Materials and methods

All reactions were performed under dry nitrogen or argon unless otherwise noted. Solvents were stored over drying agents, degassed prior to use, and vacuum-transferred into reaction mixtures. Toluene and THF were dried over sodium benzophenone ketyl, ethanol was dried over magnesium, and CH_2Cl_2 was dried over calcium hydride. The aldehydes used in the catalytic runs were freshly distilled before use. The 2-methoxy propene was passed through basic alumina to remove any acidic impurities and was then distilled. The aldehyde precursors, 4-hydroxy-3-phenanthrenecarbox-aldehyde and 1-hydroxybenz[a]anthracene-2-carboxaldehyde were synthesized by procedures we have reported previously [7]. (S)-NOBIN was synthesized from *rac*-BINOL in 98% ee using literature methods [8].

CD spectra were collected on a JASCO 720 spectropolarimeter. Solution samples for this technique was prepared using dried spectroscopic grade THF, at concentrations that ranged between 1.5 and 2.5×10^{-5} M. A 1.00 cm path length quartz cell was employed for the analysis. 1H and ^{13}C NMR spectra were obtained on a Varian Unity 400 MHz (for 1H) spectrometer employing residual solvent protons or TMS as internal standards. Crystallographic data was collected using either a Bruker SMART 1000 CCD or a Bruker-AXS SMART APEX CCD. All mass spectra were recorded Bruker Daltonics HCT Ultra ESI-Ion Trap Mass Spectrometer. IR spectra were taken of neat samples using a Nicolet 380 FT-IR spectrometer with ZnSe ATR attachment. Single point energies for minimized geometries

* Corresponding author. Tel.: +1 (785) 532 6688; fax: +1 (785) 532 6666.

E-mail address: clevy@ksu.edu (C.J. Levy).

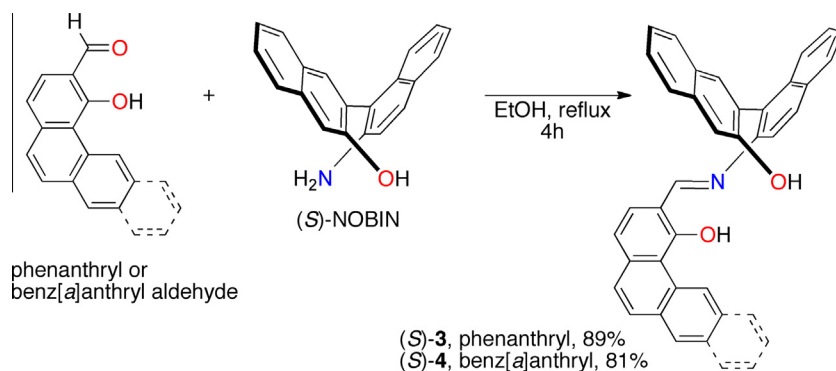


Scheme 1. Carreira's Ti(IV)-NOBIN catalyst for the asymmetric hetero-ene addition of 2-methoxypropene to aromatic, aliphatic and acetylinic aldehydes.

were calculated using GAUSSIAN 09 with the B3LYP density functional and the STO3G (d,p) basis set. Input files were generated using Arguslab.

2.1. (S)-3, (S)-2-hydroxy-1,1'-binaphthyl-2'-imine-phenanthrene-1-ol

A mixture of 0.0936 g (0.351 mmol) of (S)-NOBIN and 0.115 g (0.422 mmol) of 2-phenanthraldehyde-1-ol were refluxed in absolute ethanol (15 mL) under argon for 10 h. The mixture was hot



Scheme 2. Synthesis of ligands (S)-3 and (S)-4 by condensation.

filtered, washed with hot ethanol, and the orange solid was dried *in vacuo*. Yield of (S)-3: 0.210 g, 89% from (S)-NOBIN. Melting point = 201 °C; $[\alpha]_D^{20}$ (20 °C) = +124 ($c = 1.04$, THF). ^1H NMR (CDCl_3 , 400 MHz): δ 4.88 (s, 1H, OH); 7.12–7.14 (d, 1H, $J = 3.4$ Hz, CH); 7.26 (m, 2H, CH); 7.34–7.42 (d, 1H, $J = 3.8$ Hz, CH); 7.35 (dt, 2H, $J = 1.8$ Hz, CH); 7.36–7.42 (d, 1H, $J = 2.8$ Hz, CH); 7.42 (dt, 2H, $J = 1.8$ Hz, CH); 7.49 (d, 1H, $J = 2.8$ Hz, CH); 7.53 (m, 2H, CH); 7.56 (m, 2H, CH); 7.64 (dt, 2H, $J = 1.8$ Hz, CH); 7.75–7.77 (d, 1H, $J = 3.8$ Hz, CH); 7.83 (m, 2H, CH); 7.95–7.97 (d, 2H, $J = 3.4$ Hz, CH); 8.03 (t, 1H, $J = 2.8$ Hz, CH); 8.16–8.18 (d, 2H, $J = 3.4$ Hz, CH); 8.84 (s, 1H, CH); 9.43–9.46 (d, 1H, $J = 3.4$ Hz, CH); 14.97 (s, 1H, OH). ^{13}C NMR (CDCl_3 , 100 MHz): δ 115.14, 115.82, 117.24, 118.82, 123.74, 124.72, 125.10, 126.04, 126.63, 127.08, 127.25, 127.99, 128.32, 129.11, 129.78, 130.66, 131.00, 131.50, 132.52, 132.87, 133.79, 133.87, 137.16, 137.46, 143.72, 151.33, 160.96, 165.50. TOF-MS (m/z): $[\text{M}]^+$ Calcd for $\text{C}_{35}\text{H}_{23}\text{O}_2\text{N}_1$ 490.181, found 490.022. Anal. Calc. for $\text{C}_{35}\text{H}_{23}\text{O}_2\text{N}_1$: C, 85.87; H, 4.74; N, 2.86. Found: C, 85.10; H, 4.15; N, 2.13%.

2.2. (S)-4, (S)-2-hydroxy-1,1'-binaphthyl-2'-imine-benz[a]anthracene-1-ol

A mixture of 0.100 g (0.351 mmol) of (S)-NOBIN and 0.115 g (0.422 mmol) of 2-benz[a]anthraldehyde-1-ol were refluxed in

Table 1
Crystal data and experimental parameters for structures.

Compound ^a	(S)-4	Ti[(S)-3] ₂	Ti[(S)-4] ₂
Empirical Formula	$\text{C}_{39}\text{H}_{25}\text{NO}_2$	$(\text{C}_{35}\text{H}_{21}\text{NO}_2)_4\text{Ti}_2 (\text{C}_2\text{H}_6\text{O})_4$	$(\text{C}_{39}\text{H}_{23}\text{NO}_2)_2\text{Ti} (\text{C}_2\text{H}_6\text{O})_4$
M	539.60	2230.18	1307.34
Crystal system	triclinic	orthorhombic	orthorhombic
<i>a</i> (Å)	8.5983(8)	16.0470(7)	15.5874(14)
<i>b</i> (Å)	10.8846(12)	22.6153(10)	17.2424(16)
<i>c</i> (Å)	14.7524(15)	31.1102(15)	24.5188(17)
α (°)	94.397(4)	90.00	90.00
β (°)	97.974(4)	90.00	90.00
γ (°)	103.422(4)	90.00	90.00
Unit cell vol. (Å ³)	1321.4(2)	11290.1(9)	6589.8(10)
Space group	<i>P</i> 1	<i>P</i> 2(1)2(1)2(1)	<i>P</i> 2(1)2(1)2(1)
<i>Z</i>	2	4	4
<i>T</i> (K)	120(2)	120(2)	120(2)
Radiation	Mo K α	Mo K α	Mo K α
μ (mm ⁻¹)	0.083	0.211	0.194
<i>N</i>	21393	130183	59496
<i>N</i> _{ind}	7555	29692	17538
<i>R</i> _{int}	0.1090	0.1457	0.1901
<i>R</i> ₁ ^a (<i>I</i> > 2 σ (<i>I</i>))	0.0719	0.0756	0.0807
<i>wR</i> ₂ ^a (<i>I</i> > 2 σ (<i>I</i>))	0.1420	0.1424	0.1480
<i>R</i> ₁ (all data)	0.1622	0.1618	0.2059
<i>wR</i> ₂ (all data)	0.1719	0.1726	0.1977
Goodness-of-fit (GOF)	1.001	1.004	1.037
Flack parameter		0.03(2)	−0.01(4)

^a $R_1 = \sum ||F_o| - |F_c|| / \sum |F_o|$ for $F_o > 2\sigma(F_o)$ and $wR_2 = \{ \sum [w(F_o^2 - F_c^2)^2] / \sum [w(F_c^2)] \}^{1/2}$.

absolute ethanol (10 mL) under argon for 10 h producing a dark red solution and precipitate. The mixture was hot-filtered and washed with hot ethanol to produce a dark red solid that was dried *in vacuo*. Yield of (*S*)-**2**: 0.591 g, 81% from (*S*)-NOBIN. Melting point = 209 °C; $[\alpha]_D(20\text{ }^\circ\text{C}) = +126$ ($c = 1.04$, THF); $^1\text{H NMR}$ (CDCl_3 , 400 MHz): δ 4.91 (s, 1H, OH); 7.31 (d, 1H, $J = 3.4$ Hz, CH); 7.37 (m, 4H, CH); 7.41 (d, 1H, $J = 3.8$ Hz, CH); 7.43 (d, 1H, $J = 1.8$ Hz, CH); 7.61 (m, 4H, CH); 7.71 (d, 1H, $J = 2.8$ Hz, CH); 8.05 (m, 4H, CH); 8.20 (d, 1H, $J = 3.4$ Hz, CH); 8.31 (s, 1H, CH); 8.34 (d, 1H, $J = 3.4$ Hz, CH); 8.39 (d, 1H, $J = 2.2$ Hz, CH); 8.41 (d, 1H, $J = 2.2$ Hz, CH); 8.92 (s, 1H, CH); 9.96 (s, 1H, CH); 14.98

(s, 1H, OH). $^{13}\text{C NMR}$ (CDCl_3 , 100 MHz): δ 116.15, 116.25, 116.86, 118.03, 119.74, 123.87, 124.84, 125.66, 125.82, 126.02, 126.48, 126.74, 127.04, 127.14, 127.58, 128.00, 128.63, 128.76, 128.97, 129.60, 129.78, 129.95, 130.61, 131.12, 131.24, 131.31, 131.33, 132.85, 133.02, 133.80, 133.89, 137.33, 143.84, 151.39, 161.18, 164.04. TOF-MS (m/z): $[M]^+$ Calcd for $\text{C}_{39}\text{H}_{25}\text{O}_2\text{N}_1$ 540.184, found 540.115. Anal. Calc. for $\text{C}_{39}\text{H}_{25}\text{O}_2\text{N}_1$: C, 86.80; H, 4.67; N, 2.60. Found: C, 86.59; H, 4.51; N, 2.43%. Single crystals suitable for X-ray analysis were grown by slow diffusion of hexane into a methylene chloride solution of (*S*)-**2**.

Table 2Bond lengths, bond angles, dihedral angles, interplanar angles for $\text{Ti}[(\text{S})\text{-3}]_2$ and $\text{Ti}[(\text{S})\text{-4}]_2$.

$\text{Ti}[(\text{S})\text{-3}]_2$	Distance (Å) or angle (°)		$\text{Ti}[(\text{S})\text{-4}]_2$	Distance (Å) or angle (°)
Parameter	Molecule 1	Molecule 2	Parameter	
Ligand 1			Ligand 1	
Ti–O12	1.940(3)	1.938(3)	Ti–O12	1.878(3)
Ti–O43	1.846(3)	1.861(3)	Ti–O43	1.864(3)
Ti–N25	2.160(3)	2.167(3)	Ti–N29	2.200(4)
O12–C12	1.313(5)	1.322(5)	O12–C12	1.329(5)
O43–C43	1.355(5)	1.380(5)	O43–C43	1.352(5)
N25–C25	1.291(5)	1.297(5)	N29–C29	1.303(6)
N25–C33	1.447(5)	1.431(5)	N29–C33	1.442(6)
Ligand 2			Ligand 2	
Ti–O12'	1.949(3)	1.937(3)	Ti–O12'	1.884(3)
Ti–O43'	1.849(3)	1.837(3)	Ti–O43'	1.858(3)
Ti–N25'	2.148(3)	2.155(3)	Ti–N29'	2.219(4)
O12'–C12'	1.319(5)	1.327(5)	O12'–C12'	1.316(5)
O43'–C43'	1.357(5)	1.377(5)	O43'–C43'	1.366(5)
N25'–C25'	1.289(5)	1.296(5)	N29'–C29'	1.294(6)
N25'–C33'	1.439(5)	1.451(5)	N29'–C33'	1.452(6)
C11–Centroid ^a	3.424	3.536	C27–centroid ^e	3.438
C15–Centroid ^b	3.870	4.186	C36–centroid ^f	3.511
C11'–Centroid ^c	3.495	3.653	C27'–centroid ^g	3.302
C15'–Centroid ^d	3.677	3.841	C36'–centroid ^h	3.763
O12–Ti–N25	80.88(12)	80.56(12)	O12–Ti–N29	79.35(14)
O12–Ti–O43	169.19(12)	163.47(12)	O12–Ti–O43	100.67(14)
O12–Ti–O12'	86.31(12)	84.51(12)	O12–Ti–O12'	160.65(14)
O12–Ti–O43'	90.63(12)	89.40(12)	O12–Ti–O43'	93.17(14)
O12–Ti–N25'	88.55(12)	94.01(12)	O12–Ti–N29'	87.38(14)
N25–Ti–O43	88.76(12)	83.89(13)	N29–Ti–O43	84.62(14)
N25–Ti–O12'	87.53(12)	95.03(12)	N29–Ti–O12'	87.16(14)
N25–Ti–N25'	164.78(13)	173.46(13)	N29–Ti–N29'	91.21(14)
N25–Ti–O43'	103.94(12)	100.25(13)	N29–Ti–O43'	171.19(15)
O43–Ti–O12'	90.18(12)	91.32(12)	O43–Ti–O12'	91.71(14)
O43–Ti–N25'	100.99(13)	101.12(13)	O43–Ti–N29'	170.05(15)
O43–Ti–O43'	94.89(13)	98.90(13)	O43–Ti–O43'	101.47(14)
C12'–Ti–N25'	80.85(12)	80.75(12)	C12'–Ti–N29'	79.04(15)
C12'–Ti–O43'	167.53(12)	162.39(12)	C12'–Ti–O43'	98.92(14)
N25'–Ti–O43'	86.99(12)	83.22(13)	N29'–Ti–O43'	83.75(14)
C25–N25–C33	118.5(3)	115.3(3)	C29–N29–C33	115.5(4)
C13–C25–N25	126.7(4)	126.3(4)	C13–C29–N29	125.2(5)
C25'–N25'–C33'	117.2(3)	117.7(3)	C29'–N29'–C33'	116.7(4)
C13'–C25'–N25'	126.1(4)	125.7(4)	C13'–C29'–N29'	125.7(5)
C13–C25–N25–C33	164.8(4)	169.7(4)	C13–C29–N29–C33	–170.3(4)
C13'–C25'–N25'–C33'	165.6(4)	166.0(4)	C13'–C29'–N29'–C33'	–171.0(5)
NAP1–NAP1A ⁱ	68.87	60.78	NAP1–NAP1A ⁱ	62.69
NAP1–PHEN1 ⁱ	87.53	83.38	NAP1–BA1 ^j	71.72
NAP2–NAP2A ⁱ	63.08	61.07	NAP2–NAP2A ⁱ	63.00
NAP2–PHEN2 ⁱ	88.14	82.40	NAP2–BA2 ^j	69.40
PHEN1–PHEN2 ⁱ	11.82	10.03	BA1–BA2 ^j	69.99
			BA1–NAP2 ^j	14.58
			BA2–NAP1 ^j	13.24

^a Centroid is calculated for C11–C16 of ligand 2.^b Centroid is calculated for C11, C16–C19, C24 of ligand 2.^c Centroid is calculated for C11–C16 of ligand 1.^d Centroid is calculated for C11, C16–C19, C24 of ligand 1.^e Centroid is calculated for C31–C36 of ligand 2.^f Centroid is calculated for C19–C21, C26–C28 of ligand 2.^g Centroid is calculated for C31–C36 of ligand 1.^h Centroid is calculated for C19–C21, C26–C28 of ligand 1.ⁱ Calculated absolute value of interplanar angle. See Fig. 2 for fragment labels.^j Calculated absolute value of interplanar angle. See Fig. 4 for fragment labels.

2.3. Ti[(S)-3]₂

Slow addition of Ti(OⁱPr)₄ (0.036 mL, 0.123 mmol) at RT to a solution of the (S)-3 (0.120 g, 0.246 mmol) in 3 mL of toluene resulted in an orange-red solution. The mixture was stirred for 4 h, filtered, and the remaining solvent and volatiles were removed under reduced pressure. The resulting red solid was dried *in vacuo*. Yield of Ti[(S)-3]₂: 0.097 g, 77%. ¹H NMR (CDCl₃, 400 MHz): δ 5.98–6.01 (d, 2H, J = 4.8 Hz, CH); 6.33–6.35 (d, 2H, J = 5.2 Hz, CH); 6.56–6.59 (d, 2H, J = 4.8 Hz, CH); 6.84–6.98 (m, 16H, CH); 7.06 (t, 2H, J = 4.6 Hz, CH); 7.22–7.24 (d, 2H, J = 4.8 Hz, CH); 7.26–7.28 (d, 2H, J = 5.8 Hz, CH); 7.39 (m, 2H, CH); 7.45–7.47 (d, 2H, J = 3.2 Hz, CH); 7.52–7.53 (d, 2H, 3.2 Hz, CH); 7.58–7.60 (d, 2H, J = 3.2 Hz, CH); 7.70–7.72 (d, 2H, J = 6.8 Hz, CH); 8.13 (s, 2H, CH); 9.66–9.68 (d, 2H, J = 5.8 Hz, CH). ¹³C NMR (CDCl₃, 100 MHz): δ 116.27, 118.83, 119.68, 119.80, 119.98, 121.04, 122.41, 124.57, 125.16, 125.58, 125.76, 126.04, 126.42, 126.95, 127.12, 127.39, 127.90, 128.03, 128.15, 128.56, 129.09, 129.44, 129.50, 130.05, 130.61, 131.46, 131.65, 133.06, 133.58, 138.16, 148.37, 159.11, 163.71, 165.18, 166.28. TOF-MS (*m/z*): [M+H]⁺ Calcd for C₇₀H₄₃O₄N₂Ti 1023.2702, found 1023.2665 (3.6 ppm). IR: ν_{C=N} 1614.26 cm⁻¹, ν_{Ti-O} 523.92 cm⁻¹, ν_{Ti-N} 509.61 cm⁻¹. Single crystals suitable for X-ray analysis were grown by slow cooling of a concentrated ethanol solution.

2.4. Ti[(S)-4]₂

Slow addition of Ti(OⁱPr)₄ (0.054 mL, 0.186 mmol) at RT to a solution of the (S)-4 (0.200 g, 0.371 mmol) in 3 mL of toluene resulted in a dark red solution. The mixture was stirred for 4 h, filtered, and the remaining solvent and volatiles were removed under reduced pressure. The resulting red solid was dried *in vacuo*. Yield of Ti[(S)-4]₂: 0.160 g, 77%. ¹H NMR (CDCl₃, 400 MHz): δ 6.02–6.04 (d, 2H, J = 5.2 Hz, CH); 6.06 (t, 2H, J = 4.2 Hz, CH); 6.36–6.38 (d, 2H, J = 5.2 Hz, CH); 6.42–6.44 (d, 2H, J = 5.2 Hz, CH); 6.58 (t, 2H, J = 3.4 Hz, CH); 6.70–6.72 (d, 2H, J = 3.4 Hz, CH); 6.8 (t, 2H, J = 3.8 Hz, CH); 7.04 (t, 2H, J = 3.8 Hz, CH); 7.18–7.19 (m, 4H, CH); 7.33 (m, 2H, CH); 7.34–7.36 (d, 2H, J = 5.2 Hz, CH); 7.48–7.50 (d, 2H, J = 4.8 Hz, CH); 7.56 (m, 2H, CH); 7.56–7.64 (d, 2H, J = 4.8 Hz, CH); 7.66 (m, 4H, CH); 7.71–7.72 (d, 2H, J = 5.2 Hz, CH); 7.81–7.82 (d, 2H, J = 5.2 Hz, CH); 7.90–7.91 (d, 2H, J = 4.8 Hz, CH); 7.92 (s, 2H, CH); 8.15 (s, 2H, CH); 10.40 (s, 2H, CH). ¹³C NMR (CDCl₃, 100 MHz): δ 116.50, 119.93, 120.26, 120.60, 121.41, 121.62, 122.60, 124.44, 124.50, 125.00, 125.31, 125.73, 125.85, 126.06, 126.09, 126.26, 126.46, 126.61, 126.79, 127.17, 127.81, 128.04, 129.05, 129.30, 129.73, 130.45, 130.51, 130.68, 130.99, 131.10, 132.18, 132.52, 132.61, 133.75, 138.54, 148.70, 163.56, 164.05, 165.52. [M+H]⁺ Calcd for C₇₈H₄₇O₄N₂Ti 1123.3015, found 1123.2975 (3.6 ppm). IR: ν_{Ti-O} 546.15 cm⁻¹, ν_{Ti-N} 518.98 cm⁻¹, ν_{C=N} 1607.43 cm⁻¹. Single crystals suitable for X-ray analysis were grown by slow cooling of a concentrated ethanol solution.

2.5. Catalyzed carbonyl-ene additions (representative procedure)

Freshly prepared Ti[(S)-3]₂ (1.5 mg, 0.0014 mmol) was dissolved in 2-methoxypropene (2.00 mL, 20.9 mmol) at 0 °C and 2,6-di-*tert*-butyl-4-methylpyridine (13 mg, 0.063 mmol) was added. Benzaldehyde (16 μL, 0.15 mmol) was added and the mixture was stirred for 16 h at 0 °C. The reaction mixture was concentrated *in vacuo* and the resulting residue was treated with a

biphasic mixture of diethyl ether (5 mL) and 2 N HCl (5 mL) for 30 min. The mixture was extracted with diethyl ether (2 × 10 mL), dried over anhydrous sodium sulfate, and concentrated *in vacuo*. The mixture was chromatographed on a silica gel column with 4:1 hexanes/ethyl acetate followed by 1:1 hexanes/ethyl acetate. The β-hydroxy ketone product eluted with the more polar solvent. The pure product was isolated by removing the solvent *in vacuo* (25 mg, 70%).

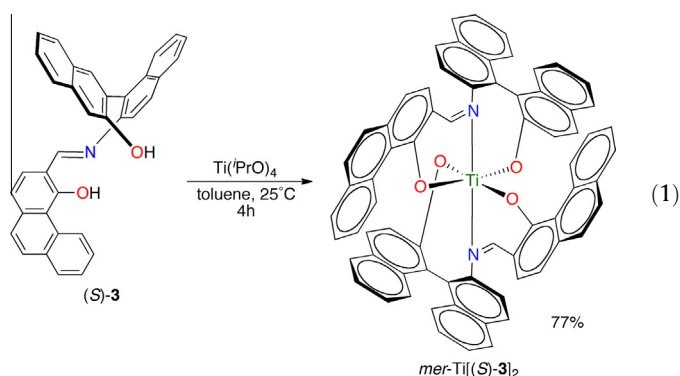
2.6. Enantiopurity determination

(*R*)-*O*-acetyl mandelic acid (20.2 mg, 0.104 mmol), carbonyl-ene product (0.104 mmol) and DMAP (2.6 mg, 0.021 mmol) were combined in 1 mL CH₂Cl₂ and cooled to 0 °C. A solution of DCC (23.7 mg, 0.115 mmol in 2 mL CH₂Cl₂) was added drop wise over 10 min. After 1 h at 0 °C the reaction was allowed to warm to room temperature and stirred for an additional hour. The precipitate was removed by filtration and the resulting solution was washed successively with 5 mL of 0.5 N HCl, 2 N Na₂CO₃ and brine. The organic layer was dried over MgSO₄, and concentrated. The crude product was purified by silica flash column chromatography with 6:1 hexane:ethyl acetate mixture. The enantiomeric excess of the product was determined by integration of the ¹H NMR resonances of the diastereomeric mandelic esters.

3. Results and discussion

3.1. Synthesis

Two new tridentate ligands, (S)-3 and (S)-4, were synthesized by the condensation of (S)-NOBIN with polyaromatic aldehydes in refluxing ethanol (Scheme 2). ¹H and ¹³C NMR are consistent with the structures and indicate high levels of purity with respect to organic contaminants. All 25 unique carbon environments are identified in the ¹³C spectrum of (S)-3, while 29 carbons were seen for (S)-4. The ligands were metallated with Ti(OⁱPr)₄ to produce neutral octahedral complexes of the type TiL₂ (Eqs. 1 and 2). After filtration, the 2-propanol side product is readily removed in the drying step. ¹H and ¹³C NMR are consistent with C₂-symmetric structures: the same number of unique carbons are seen as for the ligands, but with different chemical shifts. The NMR spectra show that each sample is comprised of a single dominant component (~90%) with minor signals corresponding to impurities or the presence of a second isomer. The molecular structures are confirmed by high-resolution mass spectrometry and X-ray structure determination on recrystallized samples.



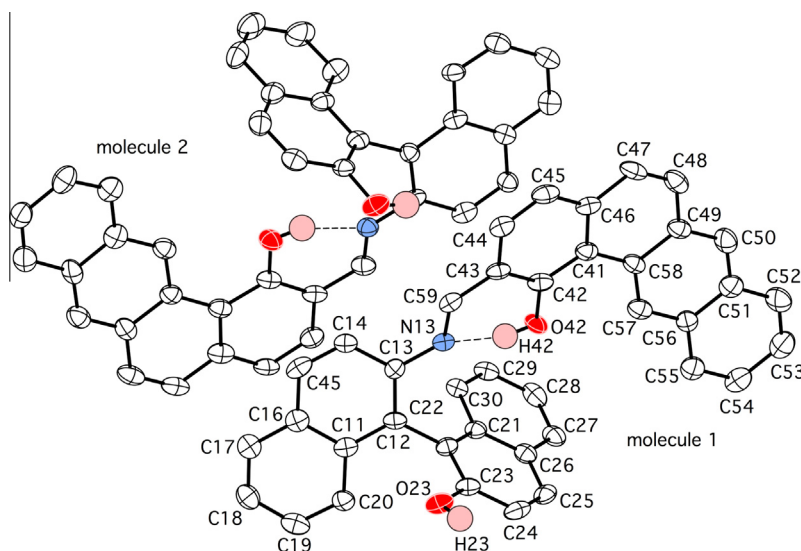
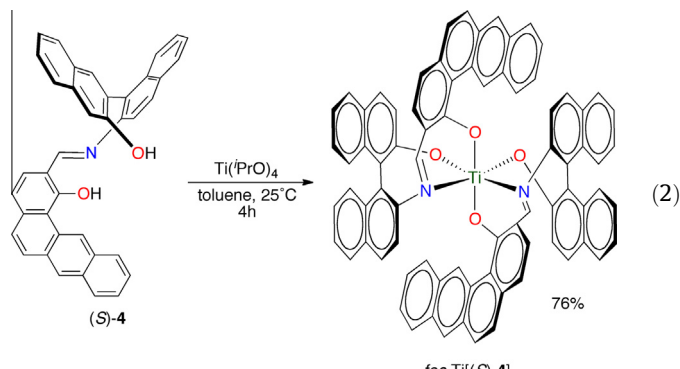


Fig. 1. Thermal ellipsoid plot (50% probability) of (*S*)-**4**. C–H hydrogens are removed for clarity. Selected bond lengths (Å): molecule 1 H42–O42 0.8400, C42–O42 1.342(5), C59–N13 1.297(6), C13–N13 1.400(6), C43–C59 1.432(7); molecule 2 H42–O42 0.8400, C42–O42 1.316(6), C59–N13 1.293(6), C13–N13 1.405(6), C43–C59 1.429(7).



3.2. Structural characterization

The crystal data for the structures are reported in Table 1. Selected bond lengths, bond angles, and other parameters are presented in Table 2.

Single crystals of the ligand (*S*)-**4** were grown by the slow diffusion of hexanes into a CH_2Cl_2 solution of the compound. There are two independent but similar molecules in the unit cell (Fig. 1). The main difference is the interplanar angle between the benz[*a*]anthryl unit and the attached naphthyl group: in molecule 1 the angle between the mean planes is 24.8° , while in molecule 2 it is 5.0° . The angle between the naphthyl groups in the molecule is comparable (72.7° and 78.8° for mean planes) and the naphthyl OH protons are involved in hydrogen bonding interactions with the imine nitrogens.

Bright orange crystals of $\text{Ti}[(\text{S})\text{-3}]_2 \cdot 2\text{C}_2\text{H}_5\text{O}$ were grown by cooling an ethanol solution of $\text{Ti}[(\text{S})\text{-3}]_2$. There are four ethanol molecules in the asymmetric unit: two are modeled at fixed positions while the other two are each disordered over two positions. The asymmetric unit has two independent, but very similar complexes (Fig. 2 shows molecule 1). Both have ligands in meridional coordination modes and have the *M* (Λ) configuration (alternately *OC*-6-22'-*A*). [9] The donors of each ligand and the metal centre are close to coplanar and the ligands are nearly perpendicular (89.29°). However, there are substantial distortions from octahedral geometry. Adjacent donors for each $\text{O}_n\text{NO}_{\text{pa}}$ (O_n = naphthyl O, O_{pa} = phenanthryl O) ligand have chelate angles significantly below

90° : $\text{N-Ti-O}_{\text{pa}}$ $80.56\text{--}80.88^\circ$ and $\text{O}_n\text{-Ti-N}$ $83.22\text{--}88.76^\circ$. All trans relationships are significantly distorted from linear: $\text{O}_n\text{-Ti-O}_{\text{pa}}$ $162.39(12)\text{--}169.19(12)^\circ$, N-Ti-N $164.78(13)$ and $173.46(13)$. The phenanthryl groups are stacked (interplanar angles of 11.82° and 10.03° for the two molecules) and involved in face-to-face $\pi\text{-}\pi$ interactions (Fig. 3). The centroid-C11/C11' distances range from $3.42\text{--}3.65$ Å consistent with attractive stacking. There are also longer centroid-C15/C15' distances associated with each molecule (range $3.68\text{--}4.12$ Å). The attached naphthyl groups are essentially perpendicular to the phenanthryl plane. The interplanar angle between the naphthyl fragments ranges from 60.78 to 68.87° , significantly smaller than in the free ligand and within the region where binaphthyl-based steric repulsions are moderate [10].

Bright red crystals of $\text{Ti}[(\text{S})\text{-4}]_2 \cdot 4\text{C}_2\text{H}_5\text{O}$ were grown by cooling an ethanol solution of $\text{Ti}[(\text{S})\text{-4}]_2$. There is a single titanium complex in the asymmetric unit (Fig. 4) along with four ethanol molecules. The ligands have facial coordination in this complex. Glowka et al. described the structures of facial bis(salicylaldiminato) complexes with $\text{O}_{\text{sal}}\text{N}_{\text{im}}\text{X}$ in terms of the cis/trans relationships of identical donors [11]. Using this descriptor we have a *cct* facial isomer.¹ This is the *OC*-6-1'3'-*C* isomer by the configuration index and *C/A* conventions. The geometry at the metal centre is distorted octahedral. Adjacent donors for each $\text{O}_n\text{NO}_{\text{ba}}$ (O_{ba} = benz[*a*]anthryl O) ligand have chelate angles significantly below 90° : $\text{N-Ti-O}_{\text{ba}}$ is near 79° and $\text{O}_n\text{-Ti-N}$ is near 84° . The angle between the terminal oxygen donors, on the other hand, is opened up by about 10° . The small chelate angles lead to a trans $\text{O}_{\text{ba}}\text{-Ti-O}_{\text{ba}}$ angle that is significantly less than linear ($160.65(14)^\circ$) with O_{ba} donors pulled toward the adjacent nitrogens. The donor atoms are significantly out of the plane defined by Ti, N29, N29', O43, and O43'. The trans donors N29 and O43' are above the plane by 0.128 and 0.140 Å, respectively, while N29' and O43 are below the plane by 0.134 and 0.147 Å, respectively. The interplanar angle between the naphthyl fragments is 62.69° , significantly smaller than in the free ligand. The benz[*a*]anthryl groups are oriented away from one another in the complex, so they are not $\pi\text{-}\pi$ stacked as in $\text{Ti}[(\text{S})\text{-3}]_2$. However, there are face to face stacking interactions between the benz[*a*]anthryl group of each ligand and one naphthyl group of another: the benz[*a*]anthryl to naphthyl angles (BA-NAP) are 14.58° and 13.24° . The four closest C-centroid

¹ Sidearm oxygen donors (O_{sal}) are cis, imine donors (N_{im}) are cis, and naphthyl oxygen donors (X) are trans: *cct*.

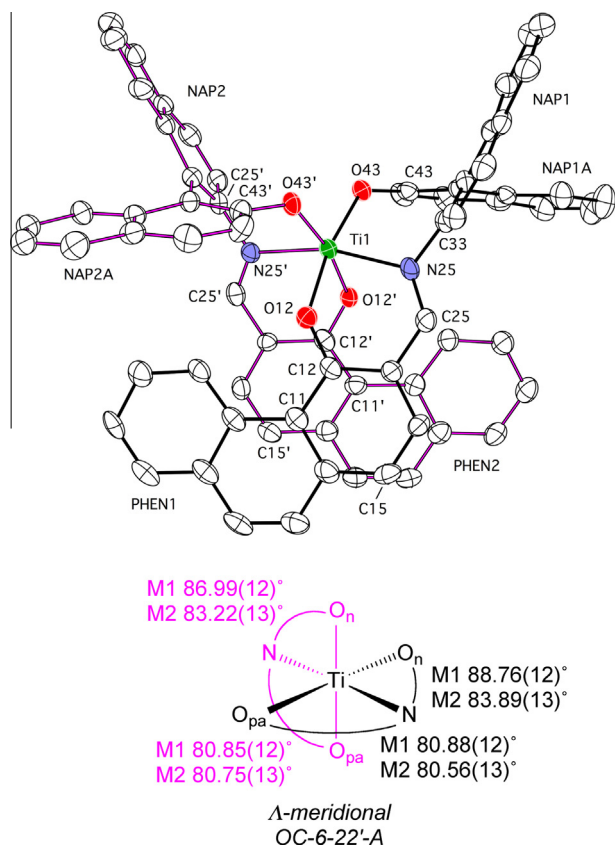


Fig. 2. Thermal ellipsoid plot (50% probability) of $\text{Ti}[(S)\text{-}3]_2$ (molecule 1). The hydrogens are removed for clarity and the two (*S*-3) ligands are indicated with different bond colors (top). Skeletal structure of complex along with cis-angles for the two molecules (M1 and M2, bottom). (Color online.)

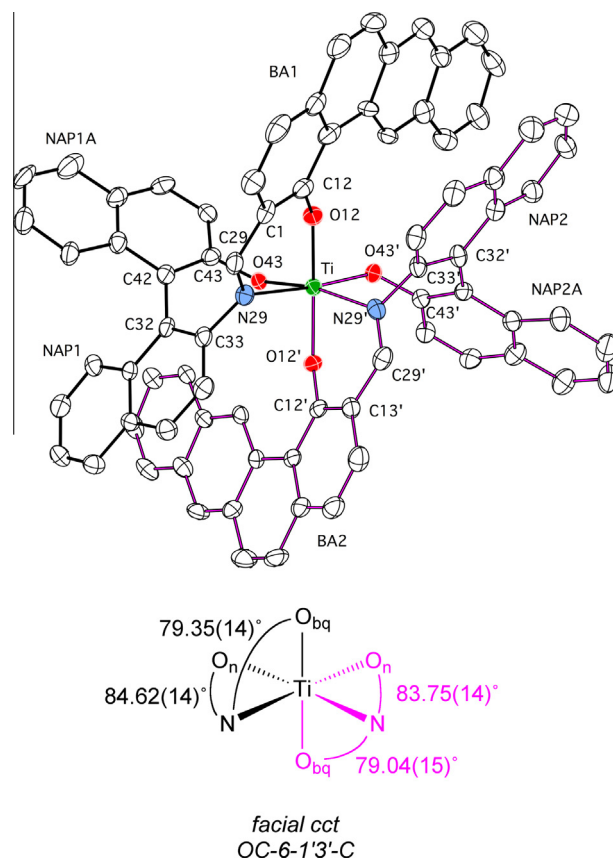


Fig. 4. Thermal ellipsoid plot (50% probability) of $\text{Ti}[(S)\text{-}4]_2$. The hydrogens are removed for clarity and the two (*S*-4) ligands are indicated with different bond colors (top). Skeletal structure of complex along with cis-angles (bottom). (Color online.)

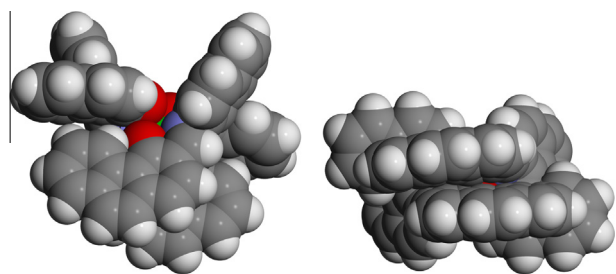


Fig. 3. Space-filling models (50% probability) of $\text{Ti}[(S)\text{-}3]_2$ (molecule 1).

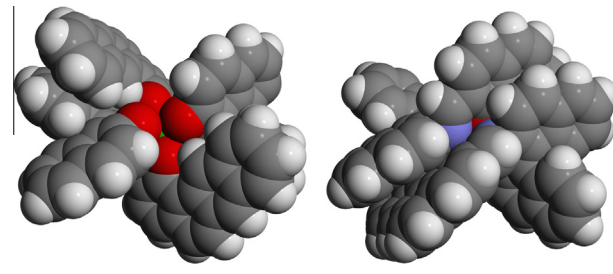


Fig. 5. Space-filling models (50% probability) of $\text{Ti}[(S)\text{-}4]_2$.

distances associated with the interactions are 3.302, 3.438, 5.511 and 3.763 Å (see Fig. 5).

The two TiL_2 structures reported here are amongst the few that have been reported for this ligand type. Chiral tridentate ligands have been produced by the condensation of NOBIN with salicylaldehydes, pyridine-2-carboxaldehyde, or pyrrolidine-2-carboxaldehyde and those that have structurally-characterized metal complexes (**6**–**11**) are illustrated in Fig. 6 (stereochemistry not indicated in structures). In several structures the ligand is only bidentate, with the naphthyl-oxygen remaining protonated and uncoordinated to the metal [12]. In complexes where the ligand is tridentate to a single metal ion its coordination is closer to trigonal than linear [5,6]. For dinuclear complexes the naphthyl-oxygen is normally bridging and the coordination of the ligand can be trigonal or linear [5,12]. The only octahedral complexes of the type ML_2 have been seen for Ti(IV) . Ding and co-workers [6] examined racemic and enantiomerically enriched **6** and found fac-TiL_2

complexes in each case, but with different coordination modes (Fig. 6). More recently, Zi and co-workers crystallographically characterized two fac-TiL_2 complexes, each with the *cct* mode observed for $\text{Ti}[(S)\text{-}4]_2$ (Fig. 6) [5c]. The meridional coordination mode seen for $\text{Ti}[(S)\text{-}3]_2$ has not previously been observed for this ligand type. However, this mode was seen with a partially reduced H_8 -NOBIN backbone [5c].

3.3. DFT calculations

The crystal structure data for $\text{Ti}[(S)\text{-}3]_2$ and $\text{Ti}[(S)\text{-}4]_2$ were used to generate input files for geometry minimization and single point energy calculations using DFT methods. Additional facial and meridional geometries of each compound were also generated in Arguslab by ligand rotation and molecular mechanics minimization. This method found four additional configurations of $\text{Ti}[(S)\text{-}3]_2$ (3 *fac* and 1 *mer*) and three additional configurations of

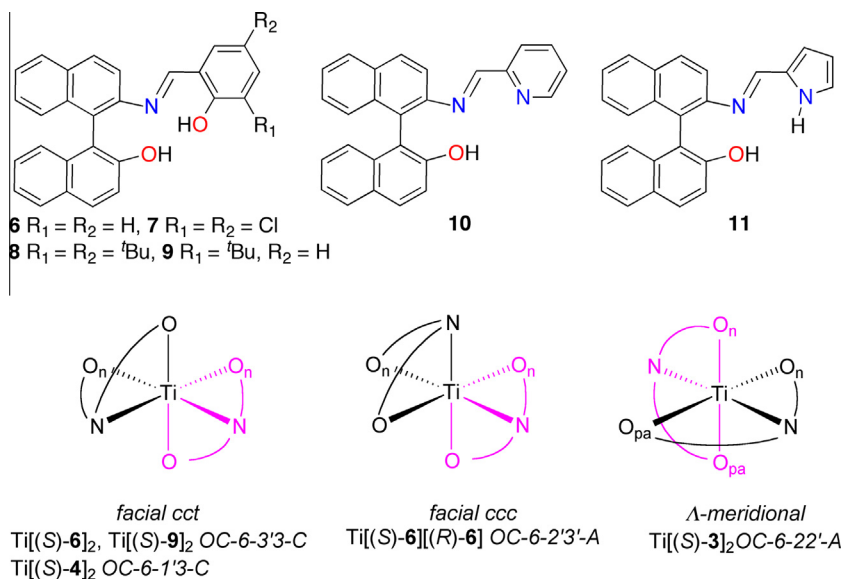


Fig. 6. Structures of NOBIN-based ligands that have structurally-characterized (X-ray) metal complexes (top). Coordination modes of TiL_2 complexes of NOBIN-based ligands (bottom).

$Ti[(S)\text{-}4]_2$ (1 *fac* and 2 *mer*). The OC-6-2'2'-A facial configuration of $Ti[(S)\text{-}4]_2$ failed to minimize without converting to another configuration. The calculations predict that the OC-6-2'2'-A meridional configuration is most stable for $Ti[(S)\text{-}3]_2$ by 24.1 kcal/mol compared to facial OC-6-3'3'-A and this agrees with the experimentally observed OC-6-2'2'-A structure (Fig. 7). The same energy ordering was seen for the calculated geometries of $Ti[(S)\text{-}4]_2$, except that OC-6-2'2'-A was absent, as noted. However, the experimentally observed OC-6-1'3'-C structure is predicted to be that with the highest energy. The discrepancy in predicted and observed configurations for $Ti[(S)\text{-}4]_2$ may be the result of π - π and packing

interactions. The low energy OC-6-2'2'-A structure does not have and significant intramolecular π - π stacking interactions and it is also a very open structure, suggesting that there may be difficulty in achieving efficient packing. These factors are not accounted for in the DFT calculations and may well drive the observed structure of $Ti[(S)\text{-}4]_2$, especially if there is facile ligand for solvent exchange in solution that allows the most stable crystal to form under equilibrium conditions.

3.4. Spectral characterization

The ligands (S)-3 and (S)-4 and their titanium(IV) complexes have well resolved 1H and ^{13}C NMR spectra that are consistent with the expected structures. In the 1H spectra of both the ligands, the intramolecularly bonded phenolic hydroxyl proton from the side-arm appears at 14.90–15.00 ppm. The imine protons ($N=C-H$) of (S)-3 and (S)-4 appear at 8.84 and 8.92 ppm respectively. The downfield signals at 9.43 ppm (doublet, (S)-3) and at 9.96 ppm (singlet, (S)-4) are for the bay region hydrogens of the ring systems. These protons are affected by edge position aromatic deshielding and anisotropic deshielding from the hydroxyl group at the nearby position [13]. The expected number and pattern of aromatic signals are observed for the ligands, even though there are a number of near-coincident signals and second-order effects on intensities. The NMR spectra of the titanium complexes are consistent with diamagnetic C_2 -symmetric compounds in solution. There are impurity signals ($\sim 10\%$) in the spectra of the powdered samples that likely correspond to incomplete reaction or the presence of isomers. The major resonances seen for $Ti[(S)\text{-}3]_2$ (21 H and 35 C environments) and $Ti[(S)\text{-}4]_2$ (23 H and 39 C environments) are seen consistent with the X-ray structural data. In general, the complexes have spectra similar to those of the ligands, but with a few notable differences. As expected, the phenolic resonances are not present in the complexes. There is also a downfield shift of the bay region proton by 0.2 ppm for $Ti[(S)\text{-}3]_2$ and 0.45 ppm for complex $Ti[(S)\text{-}4]_2$. In addition there are several significant upfield shifts of protons in the complex due to the anisotropic deshielding created by the orientation of the π -systems in the C_2 -symmetric octahedral geometry compared to the C_1 -symmetric free ligand. The 1H and ^{13}C NMR spectral data are also consistent with these structures.

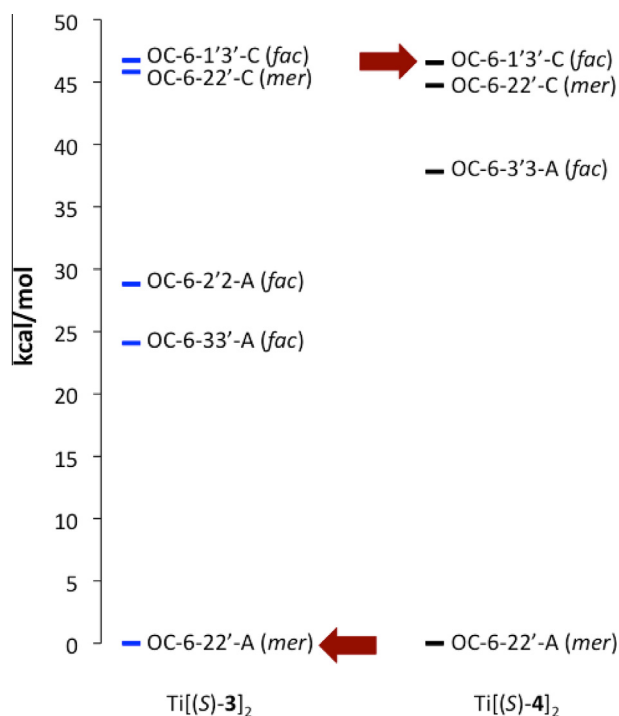


Fig. 7. DFT-calculated energies of stable configurations of $Ti[(S)\text{-}3]_2$ and $Ti[(S)\text{-}4]_2$. Crystallographically observed configurations are indicated by arrows.

In the ultraviolet range, the (*S*)-NOBIN solutions in THF display absorption spectra and circular dichroism (CD), typical for 2,2'-substituted 1,1'-binaphthyls. Systems of three absorption bands are observed, which corresponds to three basic absorption bands of β -mono-substituted naphthalene, and they can be conventionally assigned to three electron transitions of naphthalene: 1B_b , 1L_a , and 1L_b [14]. Significant circular dichroism occurs for all of these transitions. The most clearly expressed absorption band in the CD spectrum for the ligands (*S*)-**3** and (*S*)-**4** is at 235 nm and is attributed to allowed 1B_b transition of naphthyl chromophores whose rotation relative to each other is restricted. The sharp positive peak at 235 nm in the CD spectrum of the ligands is due to the presence of NOBIN with the *S* configuration. The 1L_a and 1L_b transitions in the CD spectrum for (*S*)-NOBIN generally occur at 265–340 nm range [14]. They are composed into two different wavelength ranges (265–280 nm and 310–340 nm) and both of these transitions give rise to negative peaks with small intensity in the CD spectrum. The vibronic structures in the observed absorption spectra typical of the L-transitions are expressed weakly due to the lack of symmetry in the (*S*)-NOBIN and this result in peaks with low intensity at this wavelength (265–340 nm) range.

The CD spectra of complexes $Ti[(S)\text{-}3]_2$ and $Ti[(S)\text{-}4]_2$ along with the corresponding free ligands are shown in Figs. 8 and 9, respectively. The CD peaks have shifted towards higher wavelength for both the complexes compared to the free ligands. This phenomenon can be attributed to the lowering in energy of the antibonding orbitals or the increase in energy level of the bonding orbitals after complexation [14]. The sharp positive absorption peak at 235 nm for both ligands has shifted to higher wavelengths (~20 nm) after

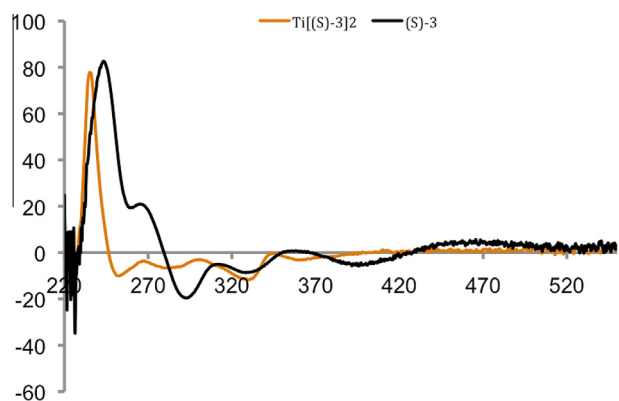


Fig. 8. CD spectra of (*S*)-**3** (orange) and $Ti[(S)\text{-}3]_2$ (black) in THF. (color online.)

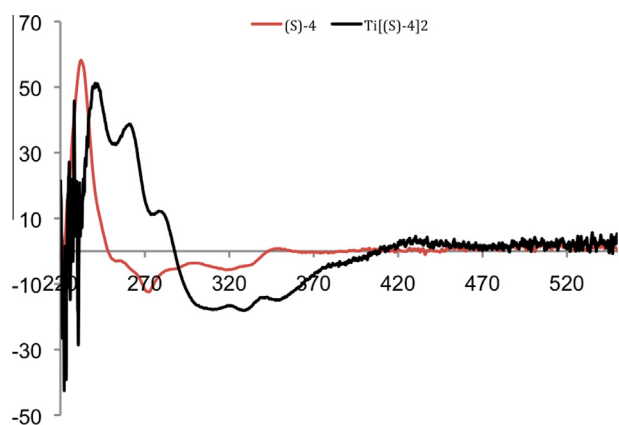
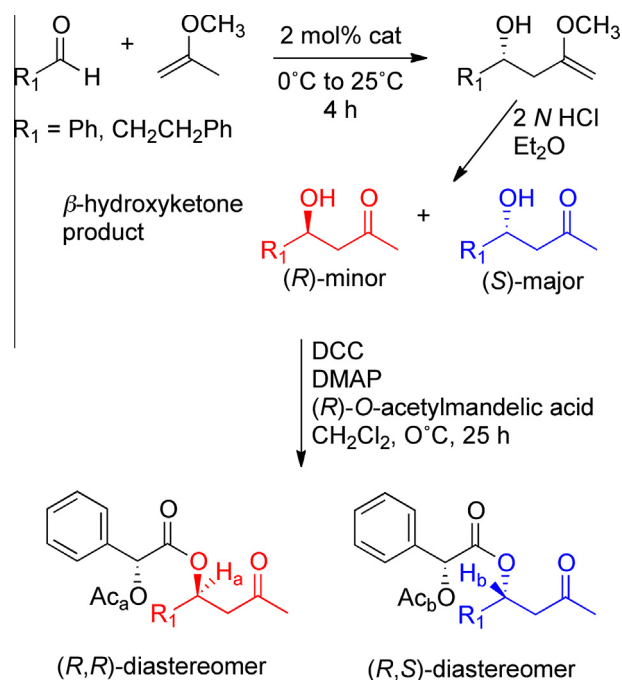


Fig. 9. CD spectra of (*S*)-**4** (red) and $Ti[(S)\text{-}4]_2$ (black) in THF. (Color online.)

complexation due to the stronger dipole–dipole interactions caused by the reduced inter planar angle between the naphthalene rings in the (*S*)-NOBIN backbone in the octahedral complexes [15]. The additional positive shoulder cotton peak at 270 nm in case of the complex $Ti[(S)\text{-}3]_2$ compared to the ligand (*S*)-**3** arise from the dipole–dipole interaction between the naphthyl ring and the phenanthryl sidearm due to the helical conformation after complexation. Also, two additional positive shoulder cotton peaks at 270 and 285 nm in case of the complex $Ti[(S)\text{-}4]_2$ compared to the ligand (*S*)-**4** arise due to the same reason as stated for the previous complex. The two negative peaks due to the L-transitions at 290 and 335 nm for complex $Ti[(S)\text{-}3]_2$ and at 335 and 350 nm for complex $Ti[(S)\text{-}4]_2$ are expressed weakly due to the complete absence of symmetry in the NOBIN backbone after complexation. The low energy broad negative peaks at 410 nm for complex $Ti[(S)\text{-}3]_2$ and at 480 nm for complex $Ti[(S)\text{-}4]_2$, arise due to the absorption by the imine bond [14].

3.5. Catalytic asymmetric carbonyl-ene condensations

The helical titanium(IV) complexes $Ti[(S)\text{-}3]_2$ and $Ti[(S)\text{-}4]_2$ are examined as catalysts for asymmetric carbonyl-ene additions between 2-methoxypropene and aromatic aldehydes (Scheme 3). Both the catalysts have coordinatively-saturated octahedral complexes, but it has been proposed that one of the ligands must dissociate to allow the titanium to act as a Lewis acid to the



Scheme 3. Carbonyl-ene addition of 2-methoxypropene with two aromatic aldehydes catalyzed by followed by $Ti[(S)\text{-}3]_2$ or $Ti[(S)\text{-}4]_2$. Derivatization with (*R*)-*O*-acetyl mandelic acid for ee determination is indicated. H_a/H_b and Ac_a/Ac_b are used as the 1H NMR markers to determine the enantiomeric excess of the product.

Table 3
Results of carbonyl-ene additions catalyzed by results by catalysts $Ti[(S)\text{-}3]_2$ or $Ti[(S)\text{-}4]_2$.

Aldehyde	Catalyst	Yield (%)	ee (%)
3-Phenylpropanaldehyde	$Ti[(S)\text{-}3]_2$	80	53
3-Phenylpropanaldehyde	$Ti[(S)\text{-}4]_2$	72	54
Benzaldehyde	$Ti[(S)\text{-}3]_2$	70	43
Benzaldehyde	$Ti[(S)\text{-}4]_2$	68	45

aldehyde [8]. Table 3 shows the results of the catalyzed addition reactions. The two compounds have similar activity and selectivity with good yields but only moderate stereoselectivities (43–54% ee). The results are somewhat better for 3-phenylpropanaldehyde than for benzaldehyde. The enantioselectivity was measured by forming an ester derivative of the β -hydroxy ketone with (*R*)-*O*-acetyl mandelic acid (Scheme 3) [16]. The chiral β -hydroxy ketone formed from the reaction of aldehyde and 2-methoxy propene reacts with (*R*)-*O*-acetyl mandelic acid in the presence of the coupling agent DCC and the catalyst DMAP. Esters with (*R,R*) and (*R,S*) configurations are formed, with the ratio depending on the enantiomeric ratio of the β -hydroxy ketone. The two protons marked as H_a and H_b as well as the methyl groups in the acetyl groups (Ac_a and Ac_b) are used as the ¹H NMR markers to determine the ratio of diastereomeric esters, and hence the ee of the β -hydroxy ketone.

4. Conclusions

In this work we have successfully synthesized two new chiral tridentate ligand based on (*S*)-NOBIN and polyaromatic aldehydes. These ligands have a distinctly different structure than those reported previously due to the extended aromatic structures. The Ti(IV) complexes of these are well characterized and reveal distinctly different coordination modes in their TiL₂ complexes. Curiously, the ligand with the most extended aromatic system, (*S*)-**4**, produces complexes that have a facial coordination that is consistent with the other reported structures with enantiopure tridentate NOBIN-based ligands [5,6]. The TiL₂ complex of (*S*)-**3** has a meridional coordination mode which has not been seen previously for similar complexes. However, it is clear that tridentate NOBIN-based ligands are not strictly trigonal-binding, as meridional coordination has been seen for MLX₂ type complexes and for ligands which bridge more than one metal [5,6,12].

Preliminary catalysis studies on the to titanium complexes illustrate activity and modest selectivity. Considerable work in looking at different substrates and examining the effects of chiral and achiral acids as additives is needed to further explore that catalytic features of these systems.

Acknowledgements

This work was supported by the National Science Foundation under grant number CHE-0349258 and by Kansas State University. Thanks to J. Tomich for use of the ECD facilities and L. Maurmann for assistance with NMR experiments. We also wish to thank Dr. Todd D. Williams, Mr. Robert Drake and Mr. Larry Seib of the KU mass spectrometry Laboratory for their efforts in acquiring the ESI spectra. Thanks to Compute Canada for the computation time.

Appendix A. Supplementary data

CCDC 959714, 959712 and 959713 contains the supplementary crystallographic data for (*S*)-**4**, Ti[(*S*)-**3**]₂ and Ti[(*S*)-**4**]₂. These data can be obtained free of charge via <http://www.ccdc.cam.ac.uk/conts/retrieving.html>, or from the Cambridge Crystallographic Data Centre, 12 Union Road, Cambridge CB2 1EZ, UK; fax: (+44) 1223-336-033; or e-mail: deposit@ccdc.cam.ac.uk. Supplementary data associated with this article can be found, in the online version, at <http://dx.doi.org/10.1016/j.poly.2014.07.001>.

References

- [1] (a) P.Y. Yang, K. Liu, M.H. Ngai, M.J. Lear, M.R. Wenk, S.Q. Yao, *J. Am. Chem. Soc.* 132 (2) (2010) 656;
(b) K. Mikami, K. Aikawa, in: I. Ojima (Ed.), *Catalytic Asymmetric Synthesis*, third Ed., John Wiley & Sons, 2010, p. 683;
(c) M. Terada, in: *Stereoselective Synthesis*, vol. 3, Thieme, 2011.
- [2] B.M. Trost, C.S. Brindle, *Chem. Soc. Rev.* 39 (2010) 1600.
- [3] (a) E.M. Carreira, R.A. Singer, W. Lee, *J. Am. Chem. Soc.* 116 (1994) 8837;
(b) E.M. Carreira, W. Lee, R.A. Singer, *J. Am. Chem. Soc.* 117 (1995) 3649;
(c) R.A. Singer, E.M. Carreira, *J. Am. Chem. Soc.* 117 (1995) 12360.
- [4] (a) K. Ding, X. Li, B. Ji, H. Guo, M. Kitamura, *Curr. Org. Synth.* 2 (2005) 499;
(b) P. Kocovsky, S. Vyskocil, M. Smrcina, *Chem. Rev.* 103 (2003) 3213.
- [5] (a) N. Zhao, Q. Wang, G. Hou, H. Song, G. Zi, *Inorg. Chem. Comm.* 41 (2014) 6;
(b) N. Zhao, Q. Wang, G. Hou, H. Song, G. Zi, *J. Organomet. Chem.* 754 (2014) 51;
(c) L. Chen, N. Zhao, Q. Wang, G. Hou, H. Song, G. Zi, *Inorg. Chim. Acta* 402 (2013) 140;
(d) N. Zhao, L. Chen, W. Ren, H. Song, G. Zi, *J. Organomet. Chem.* 712 (2012) 29;
(e) Q. Wang, L. Xiang, H. Song, G. Zi, *J. Organomet. Chem.* 694 (2009) 691;
(f) Q. Wang, L. Xiang, G. Zi, *J. Organomet. Chem.* 693 (2008) 68;
(g) G. Zi, Q. Wang, L. Xiang, H. Song, *Dalton Trans.* (2008) 5930.
- [6] (a) Y. Yuan, X. Li, J. Sun, K. Ding, *J. Am. Chem. Soc.* 124 (2002) 14866;
(b) Z.-K. Li, Y. Li, L. Lei, C.-M. Che, X.-G. Zhou, *Inorg. Chem. Commun.* 8 (2005) 307.
- [7] (a) A.V. Wlznycia, J. Desper, C.J. Levy, *Chem. Commun.* (2005) 4693;
(b) A.V. Wlznycia, J. Desper, C.J. Levy, *Dalton Trans.* (2007) 1520.
- [8] (a) Y. Yuan, J. Long, J. Sun, K. Ding, *Chem. Eur. J.* 8 (2002) 5033;
(b) K. Ding, X. Li, B. Ji, H. Guo, M. Kitamura, *Curr. Org. Syn.* 2 (2005) 499;
(c) K. Ding, Y. Wang, H. Yun, J. Liu, Y. Wu, M. Terada, Y. Okubo, K. Mikami, *Chem. Eur. J.* 5 (1999) 1734.
- [9] (a) N.G. Connelly, T. Damhus, R.M. Hartshorn, A.T. Hutton, *Nomenclature of Inorganic Chemistry – IUPAC Recommendations 2005*, RSC Publishing, 2005.;
(b) R.S. Cahn, S. Ingold, V. Prelog, *Angew. Chem., Int. Ed.* 5 (1966) 385;
(c) V. Prelog, G. Helmchen, *Angew. Chem., Int. Ed.* 21 (1982) 567.
- [10] L.D. Bari, G. Pescitelli, P. Salvadori, *J. Am. Chem. Soc.* 121 (1999) 7998.
- [11] M.L. Glowka, A. Olczak, J. Karolak-Wojciechowska, E. Ciechanowska-Urbanska, *Acta. Crystallogr., Sect. B* 54 (1998) 250.
- [12] (a) H. Brunner, F. Henning, M. Weber, M. Zabel, D. Carmona, F.J. Lahoz, *Synthesis* (2003) 1091;
(b) L. Xu, Q. Shi, X. Li, X. Jia, X. Huang, R. Wang, Z. Zhou, Z. Lin, A.S.C. Chan, *Chem. Commun.* (2003) 1666;
(c) X.-G. Zhou, J.-S. Huang, Z.-Y. Zhou, K.-K. Cheung, C.-M. Che, *Inorg. Chim. Acta* 331 (2002) 194;
(d) B. Ji, X. Han, *Cryst. Res. Technol.* 42 (2007) 926.
- [13] (a) K.L. Platt, F. Oesch, *J. Org. Chem.* 47 (1982) 5321. and references therein;
(b) R.M. Letcher, *Org. Magn. Res.* 16 (2005) 220.
- [14] E.P. Studentsov, O.V. Piskunova, A.N. Skvortsov, N.K. Skvortsov, *Russian J. Gen. Chem.* 79 (2009) 962.
- [15] I. Hanazaki, H. Akimoto, *J. Am. Chem. Soc.* 94 (1972) 4102.
- [16] K.M. Sureshan, T. Miyasou, S. Miyamori, Y. Watanabe, *Tetrahedron Asymmetry* 15 (2004) 3357.